Available online at www.CivileJournal.org

Civil Engineering Journal

(E-ISSN: 2476-3055; ISSN: 2676-6957)

Vol. 11, No. 11, November, 2025

Sizing Optimization of Trusses Using Elitist Stepped Distribution Algorithm

Mehmet Türkezer [1], Murat Altun [2, 3], Onur Pekcan [2, 3*], Oğuzhan Hasançebi [3]

[1] *Maseeh Department of Civil, Architectural, and Environmental Engineering, The University of Texas at Austin, Austin, TX 78712, United States.*

[2] *Research Center for Built Environment and Design, Middle East Technical University, Ankara, 06800, Türkiye.*

[3] *Department of Civil Engineering, Middle East Technical University, Ankara, 06800, Türkiye.*

Received 24 May 2025; Revised 17 October 2025; Accepted 23 October 2025; Published 01 November 2025

Abstract

This study investigates the efficiency of the recently developed Elitist Stepped Distribution Algorithm (ESDA) as a metaheuristic framework for truss sizing optimization. ESDA builds upon the Cross-Entropy Method by introducing an elitist stepped sampling strategy that improves the balance between exploration and exploitation during the search process. To evaluate its effectiveness, ESDA is applied to a comprehensive test suite comprising seven benchmark truss optimization problems that cover a wide range of sizes, design variables, loading conditions, and constraint types. In all cases, the objective is to minimize structural weight while satisfying stress, displacement, and stability requirements. Numerical experiments are conducted with the proposed method, and the results are compared with those algorithms reported in the literature. The findings show that ESDA attains new best or near-best solutions for large-scale problems such as the 117-bar cantilever, 130-bar transmission tower, 354-bar dome, and 942-bar tower trusses, while also producing competitive results for the 25-bar, 72-bar, and 200-bar structures with relatively modest computational effort. The novelty of this work lies in demonstrating the robustness, efficiency, and scalability of ESDA across diverse benchmarks, highlighting its potential for future structural optimization applications.

Keywords: Truss Sizing Optimization; Truss Structures; Elitist Stepped Distribution Algorithm; Metaheuristics.

1. Introduction

Design optimization has long been recognized as a fundamental component of engineering practice, providing systematic methodologies to achieve superior performance while minimizing material consumption, structural weight, and overall cost [1]. Beyond economic considerations, optimization also facilitates compliance with safety regulations, serviceability requirements, and aesthetic demands, which are central to the realization of reliable and sustainable engineering systems [2]. While design optimization has been extensively applied in fields such as aerospace and mechanical engineering, where standardized components and mass production are prevalent, its application in civil engineering presents unique challenges. Civil engineering structures, particularly large-scale infrastructures such as bridges, towers, and frames, are typically bespoke projects with complex geometries and diverse loading scenarios. Consequently, optimization in this field has predominantly focused on reducing structural cost and weight without compromising safety or code compliance. Within structural optimization, the truss sizing problem has become a classical and widely adopted benchmark. Trusses are fundamental structural systems that combine analytical simplicity with the essential challenges of more complex structures, including geometric nonlinearity, discrete design variables, and the

* Corresponding author: opekcan@metu.edu.tr

http://dx.doi.org/10.28991/CEJ-2025-011-11-05

high dimensionality arising from large numbers of members. Benchmark truss structures are therefore frequently employed to test and compare optimization algorithms. Although simplified relative to full-scale structural systems, optimal truss designs provide valuable insights during preliminary design stages and serve as effective platforms for assessing new computational methods [3].

Traditional deterministic optimization methods, including linear and nonlinear programming techniques, have historically been applied to such problems. However, the inherent nonlinearity, nonconvexity, and discrete nature of truss design often render deterministic approaches computationally demanding and highly sensitive to initial assumptions [4]. Their tendency toward premature convergence and difficulty in handling complex design constraints limit their applicability, particularly for large-scale truss systems where the search space expands rapidly with the number of members. To address these limitations, researchers have increasingly adopted metaheuristic algorithms, which rely on stochastic search processes inspired by natural, biological, or physical phenomena. Unlike deterministic methods, metaheuristics do not require gradient information and demonstrate stronger global search capabilities, enabling their application to both discrete and continuous optimization problems [5]. Representative approaches include evolutionary approaches such as Genetic Algorithms (GA) [6] and Differential Evolution (DE) [7]; swarm-based methods such as Particle Swarm Optimization (PSO) [8] and Ant Colony Optimization (ACO) [9]; and physics-based methods such as Simulated Annealing (SA) [10]. In recent decades, numerous new metaheuristics have been developed, recognizing that no single algorithm consistently outperforms others across all problem domains [11]. Examples include Big Bang-Big Crunch (BB-BC) [12], Adaptive Dimensional Search (ADS) [5], Nuclear Fission-Nuclear Fusion (N2F) [13], Grey Wolf Optimizer (GWO) [14], and Cuckoo Search (CS) [15]. Moreover, hybrid metaheuristics have been developed to combine the strengths of different algorithms and mitigate their weaknesses. Examples include Heuristic Particle Swarm Optimization (HPSO) [16], Hybrid Big Bang–Big Crunch optimization (HBB-BC) [17], Hybrid Harmony Search (HSS) [18], Heuristically Seeded Genetic Algorithm (HSGA) [19], Heuristic Particle Swarm Ant Colony Optimization (HPSACO) [20], and Improved Flower Pollination Algorithm (IFPA) [21].

Despite extensive research applying metaheuristics to truss sizing optimization, fundamental challenges persist with respect to the scalability of algorithms to large and high-dimensional design spaces, the effective incorporation of design constraints into the optimization process, and the avoidance of premature convergence. Many established algorithms perform well on benchmark trusses with grouped variables but often lose efficiency or reliability as problem dimensionality increases, resulting in excessive computational costs or suboptimal convergence. Furthermore, the consistent integration of code-based design constraints, such as those prescribed by engineering standards, remains a demanding task that has not been fully addressed. These limitations continue to motivate the exploration of alternative metaheuristic frameworks that can provide robust convergence behavior and enhanced scalability.

Elitist Stepped Distribution Algorithm (ESDA) has been proposed as a distribution-based optimization method that builds upon the Cross Entropy Method (CEM) [22]. By applying stepped parameter settings to elite samples, ESDA introduces a more robust sampling scheme that enhances the balance between exploration and exploitation, while the elitist strategy mitigates premature convergence. In addition, its distribution-based structure improves scalability, enabling effective performance in high-dimensional search spaces. These features position ESDA as a promising yet unexplored candidate for structural optimization, with the potential to overcome persistent limitations of existing metaheuristics in large-scale, discrete, and constrained truss design. Nevertheless, its effectiveness in structural engineering applications has not yet been systematically investigated, which constitutes a critical gap in the current literature. To address this gap, the present study introduces the first comprehensive application of ESDA to truss sizing optimization. The algorithm is integrated with a finite element–based structural analysis framework and evaluated on a diverse set of benchmark problems—including the 25-bar, 72-bar, 117-bar cantilever, 130-bar transmission tower, 200-bar, 354-bar braced dome, and 942-bar tower trusses—under multiple loading and code-based constraints. The practical relevance of the study is further demonstrated by (i) optimizing large-scale structures with and without member grouping, (ii) employing discrete design variables, (iii) addressing multiple loading conditions, and (iv) enforcing American Institute of Steel Construction (AISC) specifications for both Allowable Stress Design (ASD) and Load and Resistance Factor Design (LRFD). The remainder of this paper is organized as follows: Section 2 presents the problem formulation and ESDA-based methodology, Section 3 reports the optimization results and comparative analysis, and Section 4 concludes with the key findings and implications.

2. Methodology

2.1. Sizing Optimization of Truss Structures

The objective of truss sizing optimization is to determine the cross-sectional areas of truss members that minimize the overall weight of the structure, which is often associated with cost. An optimal solution is achieved by satisfying design constraints, such as the maximum allowable stress in members (i.e., bars) and the displacements at nodes (i.e., joints). The mathematical formulation can be expressed as follows:

For a truss structure composed of I bars, and J joints, the goal is to determine the vector A, given in Equation 1, which represents the cross-sectional areas of bars, to minimize the objective function W denoting the overall weight of the truss structure, as defined in Equation 2.

$$A = [A_1, A_2, \ldots, A_I] \tag{1}$$

$$W = \sum_{i=1}^{I} \rho_i L_i A_i \tag{2}$$

where ρ_i, L_i, and A_i denote the material density, length, and cross-sectional area of the bar i, respectively. The objective function W is subjected to the following design constraints specified in equations 3 and 4.

$$g_i = \frac{\sigma_i}{(\sigma_i)_{all}} - 1 \leq 0; i = 1, \ldots, I \tag{3}$$

$$s_{j,k} = \frac{\delta_{j,k}}{(\delta_{j,k})_{all}} - 1 \leq 0; j = 1, \ldots, J \tag{4}$$

where σ_i and $\delta_{j,k}$ represent the stress in each bar, and the displacement of each joint in each direction applicable, respectively, with $(\sigma_i)_{all}$ and $(\delta_{j,k})_{all}$ indicating their maximum allowable values [4].

The constraints are handled through a penalty function approach [23] where a penalized objective function, also referred to the fitness function ϕ, is formulated as follows:

$$\phi = (W)(\Psi_p) \tag{5}$$

$$\Psi_p = \left[1 + \alpha\left(\sum_{i=1}^{I} g_i + \sum_{j=1}^{J} \sum_{k=1}^{2or3} s_{j,k}\right)\right] \tag{6}$$

where Ψ_p is the penalized weight function, and α is the penalty coefficient employed to adjust the magnitude of penalization. The maximum value of index k depends on the spatial dimension of the problem, which may be either two-dimensional or three-dimensional [3, 24].

2.2. AISC Provisions

In accordance with the AISC-ASD design code [25], the tensile stress in a truss member must not exceed the lesser of the values determined by Equation 7, where F_y and F_u denote the yield and ultimate tensile strength, respectively.

$$(\sigma_t)_{all} = \min(0.60F_y, 0.50F_u) \tag{7}$$

The maximum allowable compressive stress is determined by using Equations 8 and 9, where K_i, L_i and r_i represents the effective length factor (K_i=1), the length, and the minimum radius of gyration of the bar i, respectively. In these equations, E denotes the modulus of elasticity, while λ_i and C_c specify the slenderness ratio and critical slenderness ratio, respectively, which are calculated using Equations 10 and 11.

$$(\sigma_c)_{all} = \frac{\left[1 - \frac{\left(\frac{K_i L_i}{r_i}\right)^2}{2C_c^2}\right] F_y}{\frac{5}{3} + \frac{3\left(\frac{K_i L_i}{r_i}\right)}{8C_c} - \frac{\left(\frac{K_i L_i}{r_i}\right)^3}{8{C_c}^3}}, \lambda_i < C_c \text{ (Inelastic buckling)} \tag{8}$$

$$(\sigma_c)_{all} = \frac{12\pi^2 E}{23\left(\frac{K_i L_i}{r_i}\right)^2}, \lambda_i \geq C_c \text{ (Elastic buckling)} \tag{9}$$

$$\lambda_i = \frac{K_i L_i}{r_i} \leq 300 \text{ for members in tension} \qquad \lambda_i = \frac{K_i L_i}{r_i} \leq 200 \text{ for members in compression} \tag{10}$$

$$C_c = \sqrt{\frac{2\pi^2 E}{F_y}} \tag{11}$$

The AISC-LRFD [26] design code defines the nominal tensile strength P_n as the product of F_y (the yield strength) and A_g (the gross cross-sectional area of a bar), as shown in Equation 12.

$$P_n = F_y A_g \tag{12}$$

The nominal compressive strength, shown in Equation 13, is determined by multiplying A_g, by F_{cr} (the critical stress associated with flexural buckling). The calculation of F_{cr} is shown in Equations 14 and 15.

$$P_n = F_{cr} A_g \tag{13}$$

$$F_{cr} = \left(0.658^{\lambda_c{}^2}\right) F_y \; if \; \lambda_c = \frac{K\boldsymbol{L}}{r\pi}\sqrt{\frac{F_y}{E}} \leq 1.5 \tag{14}$$

$$F_{cr} = \left(\frac{0.877}{\lambda_c{}^2}\right) F_y, \lambda_c = \frac{K\boldsymbol{L}}{r\pi}\sqrt{\frac{F_y}{E}} > 1.5 \tag{15}$$

2.3. Elitist Stepped Distribution Algorithm

Introduced by Altun & Pekcan [27], ESDA is a metaheuristic algorithm that leverages the core algorithmic structure of CEM to improve the search capabilities of distribution-based search algorithms. The improvements primarily focus on the distribution procedure, specifically on how the distribution parameters are updated. By enhancing the exploration and exploitation capabilities of CEM, ESDA is tailored to reduce the possibility of premature convergence to local optima by generating a large set of elite candidate solutions.

ESDA has three main subroutines: (i) initialization, (ii) updating distribution parameters (including the center of the distribution and its standard deviation), and (iii) updating positions using a normal distribution. To illustrate, consider a function *F(x)* with *I* design variables, to be minimized, where the position vector of n^{th} sample is represented as $\boldsymbol{X^n} = [x_1^n, x_2^n, \dots, x_I^n]$. In the first part, the algorithm performs a uniformly randomized distribution-based initialization as shown in Equation 16. Here, a random solution is generated using the random function *rand* between the lower (x_i^{min}) and upper bound (x_i^{max}) of each bar, where *i* denotes the i^{th} design variable (cross-sectional area of the bar *i*). This subroutine is performed for all samples.

$$x_i^n = x_i^{min} + rand(x_i^{max} - x_i^{min}) \tag{16}$$

Second, the center of the distribution and deviation for each bar are updated based on the elite samples. To determine the elite samples for each iteration, the fitness value of each sample *n* is evaluated using the objective function at iteration *t*, $fit^n(t) = F(X^n(t))$. The samples are then sorted according to their fitness values, from the best to the worst solution. Using the sorted solutions, $\bar{\boldsymbol{X}}^{\boldsymbol{n}} = [\bar{x}_1^n, \dots, \bar{x}_i^n, \dots, \bar{x}_I^n]$, two different elite sets are determined by employing two distinct elite percentage parameters of ESDA, p_1 and p_2. The first elite set is selected among the best K_{mean} samples to compute the center of the deviation, where K_{mean} is the integer value obtained by multiplying p_1 and *K*. As shown in Equation 17, the distribution center, μ_i, is calculated by using a fitness-weighted mean of the elite set, with better fitness values contributing more significantly to the result. On the other hand, the second elite set is composed of the first p_2 percent of the sorted solutions, denoted as K_{std}. Using these samples, first, a mean position vector, $\tilde{\mu}_i$, is calculated for each bar *i*, as shown in Equation 18; then, the standard deviation of the elite samples for each dimension, σ_i, is determined using Equation 19.

$$\mu_i(t+1) = \frac{\sum_{n=1}^{K_{mean}} \frac{\bar{x}_i^n}{fit^n(t)}}{\sum_{n=1}^{K_{mean}} \frac{1}{fit^n(t)}} \tag{17}$$

$$\tilde{\mu}_i(t) = \sum_{i=1}^{K_{std}} \frac{\bar{x}_i^n}{K_{std}} \tag{18}$$

$$\sigma_i(t+1) = \sqrt{\frac{\sum_{t=1}^{K_{std}} (\tilde{\mu}_i(t) - \bar{x}_i^n)}{K_{std} - 1}} \tag{19}$$

In the last sub-routine of ESDA, after incrementing the iteration t=t+1, new position vectors for each sample are generated by applying the mean and the standard deviation within a normal distribution scheme given in Equation 20. In this equation, the function *randn* is a function that returns normally distributed random variables with parameters N(0,1), as explained previously.

$$x_i^n(t) = \mu_i(t) + randn \; \sigma_i(t) \tag{20}$$

After generating a solution for each sample n in each iteration t, the algorithm checks boundary conditions, and calculates the fitness value based on the objective function. At the end of each iteration, the algorithm updates the best feasible solution by comparing the current best fitness value with that of the previous iteration. The overall procedure of ESDA, as applied to truss sizing optimization, is illustrated in the flowchart presented in Figure 1.

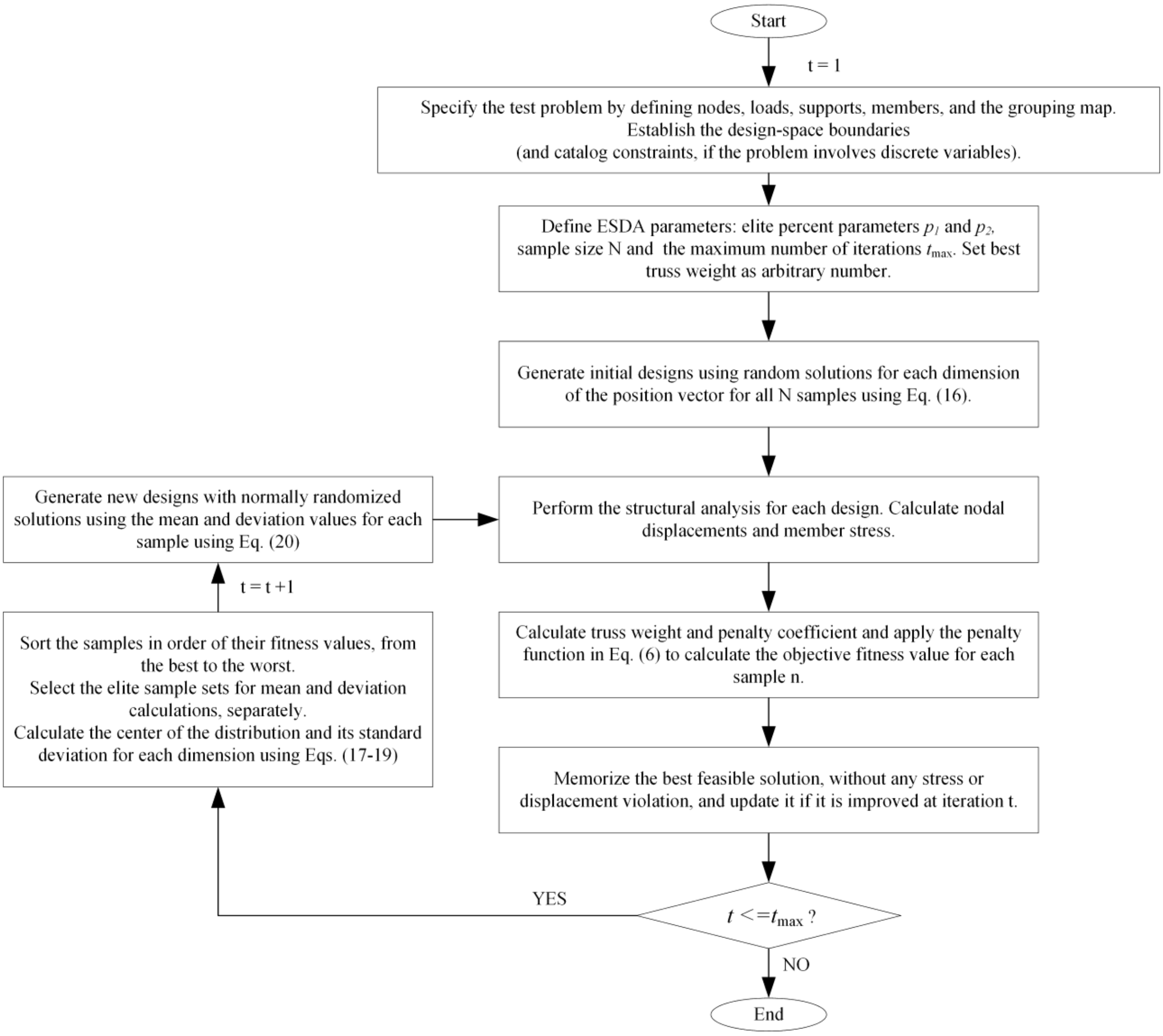

Figure 1. Flowchart of ESDA-based truss sizing optimization

3. Numerical Examples

The performance of ESDA in truss sizing optimization is evaluated through seven design problems. The four ones are established benchmark examples from the literature with grouped design variables: (i) 25-bar truss, (ii) 72-bar truss under two different loading cases, (iii) 200-bar truss, and (iv) 942-bar tower truss. The remaining three examples correspond to practically applicable truss design examples in compliance with AISC-ASD and AISC-LRFD provisions without member grouping: (i) 117-bar cantilever truss, (ii) 130-bar transmission tower truss, and (iii) 354-bar braced dome truss. For the 942-bar tower truss and one case of the 72-bar truss examples, optimization is performed within a continuous design domain, whereas for the other cases, truss member sizes are selected from a discrete set of readily available sections. The selection of these examples aims to: (i) assess the algorithm's efficiency across a variety of design variables, loading conditions, and displacement constraints; and (ii) evaluate its robustness across sizing problems with various scales, both with and without grouped design variables.

Due to the stochastic nature of metaheuristics [28], ESDA was executed 30 times independently for each example to assess the algorithm's statistical performance. The best and worst solutions, along with the mean and standard deviation, are presented for each problem, along with the number of function evaluations (NFEs), calculated as the product of the number of iterations and sample (population) size. As the number of design variables increases, design problems become more complex. Accordingly, the number of iterations and sample size are adjusted to gradually increase NFEs, mitigating premature convergence, controlling computational cost, and improving solution quality. The adjustments made for each problem are reported in Table 1. The *elite percent* parameters, p_1 and p_2, are set to 0.05 and 0.5, respectively, as recommended by the original study [27]. This selection is experimentally validated through comprehensive testing across multiple benchmark problems, showing an optimal exploration-exploitation balance with robust convergence. The penalty coefficient α is selected from a discrete set of values {0.5, 1.0, 1.5}. Initially set to 1.0, α is adjusted dynamically based on the algorithm's performance such that it is increased when the algorithm tends to approach the infeasible solution domain, and decreased to accelerate convergence towards solutions near the boundary of the feasible domain.

Table 1. Parameter settings of ESDA for the test problems

Example	Number of Design Variables	Number of Iterations	Population Size	Number of Analyses
25-Bar Truss	8	50/25	100/200	5000
72-Bar Truss	16	50/150	100	5000/15000
200-Bar Truss	29	100	100	10000
117-Bar Cantilever Truss	117	250	200	50000
130-Bar Transmission Tower	130	250	200	50000
354-Bar Truss Dome	354	500	400	200000
942-Bar Tower Truss	59	250	400	100000

3.1. Example 1: 25-Bar Truss

The 25-bar truss, depicted in Figure 2, is a widely studied benchmark problem for testing metaheuristic algorithms in structural optimization. While various versions of this problem appear in the literature, this study considers a specific case with an elastic modulus of 10,000 ksi and a material density of 0.1 lb/in³. The structure has 8 design variables, which are selected from a set of 29 discrete sections (in^2), S = [0.1, 0.2, ..., 2.4, 2.6, 2.8, 3.0, 3.2, 3.4]. The maximum allowable stress for members in both compression and tension is 40 ksi. The displacement of all nodes in the x, y, and z directions is limited to 0.35 in. A single load case is applied, with the specific loads detailed in Table 2.

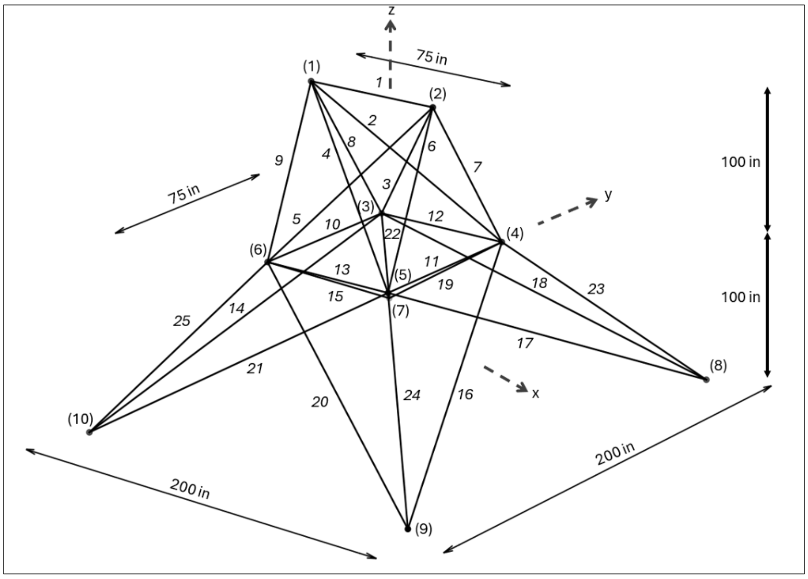

Figure 2. Schematic of the 25-bar truss

Table 2. Loads acting on the 25-bar truss

Joint	Loads (kips)		
	x	y	z
1	1.0	-10.0	-10.0
2	0.0	-10.0	-10.0
3	0.5	0.0	0.0
6	0.6	0.0	0.0

The discrete sizing optimization of the 25-bar truss structure has been investigated using a variety of metaheuristic approaches in previous studies [4, 16, 18, 19, 29–43]. In this paper, ESDA was applied to this problem, and its performance is compared in Tables 3 and 4. Table 3 presents the cross-sectional areas, minimum weights, and the number of function evaluations required to achieve these results using various metaheuristics, including ESDA. A more in-depth statistical analysis is presented in Table 4, which compares the best and worst results alongside the mean values and standard deviations (SD) for each algorithm, thereby providing a comprehensive assessment of their performance. ESDA was executed 30 times to obtain the reported results, initially configured with a sample size of 100 and 50 iterations. During this execution, ESDA successfully reached the optimum solution (i.e., 484.85 lb) reported in the literature by the 16th iteration, while using a comparatively lower number of function evaluations. However, it was noted that in more than half of the runs, the algorithm became trapped in a local optimum of 485.04 lb, resulting in a mean value of 484.95 lb. To enhance the algorithm's performance, the number of iterations and sample size were subsequently adjusted to 25 and 200, respectively. This modification reduced the number of solutions that became trapped in local optima and improved the mean value, as shown in Table 4. As inferred from comparison tables, most of the algorithms presented successfully locate the global optimum. However, as shown in Table 3, ESDA significantly outperforms the convergence speed of ABC [41], BI [30], PSO [4], ACO [31], and BB-BC [32], and even reaches the optimum slightly faster than PSO. As reported in Table 4, ESDA produces solutions that are not only accurate and consistent but also computationally efficient. Compared to most algorithms that achieve the optimum solution [4, 16, 18, 30–33, 35, 36, 38, 39, 41, 43], ESDA exhibits a better performance in terms of the consistency of solutions across different runs, with the exceptions of DE [37] and DAJA [40]. Although DE [37] achieves a mean accuracy comparable to that of ESDA, it requires a significantly higher number of function evaluations — up to 40,000 — to achieve similar results. While DAJA [40] provides perfect consistency with zero deviation, ESDA achieves near-optimal mean results using only one-fifth of the function evaluations required by DAJA [40], ensuring both computational efficiency and high accuracy. Compared to alternatives such as IWOA [43] and MBA [39], which also show strong reliability but at higher costs, ESDA delivers a superior balance of solution quality, stability, and efficiency, establishing itself as a robust tool for structural optimization.

Table 3. Comparison of different designs for the 25-bar truss problem

Variable Index	Members	GA [29]	TS [4]	ABC [41]	BI [30]	PSO [4]	ACO [31]	BB-BC [32]	ESDA
1	1	0.1	0.1	0.1	0.1	0.1	0.1	0.1	**0.1**
2	2-5	0.5	0.4	0.3	0.3	0.3	0.3	0.3	**0.3**
3	6-9	3.4	3.4	3.4	3.4	3.4	3.4	3.4	**3.4**
4	10,11	0.1	0.1	0.1	0.1	0.1	0.1	0.1	**0.1**
5	12,13	1.5	1.8	2.1	2.1	2.1	2.1	2.1	**2.1**
6	14-17	0.9	0.9	1	1	1	1	1	**1**
7	18-21	0.6	0.6	0.5	0.5	0.5	0.5	0.5	**0.5**
8	22-25	3.4	3.4	3.4	3.4	3.4	3.4	3.4	**3.4**
	Best (lb)	486.29	485.57	484.85	484.85	484.85	484.85	484.85	**484.85**
	NFEs	N/A	1626	24250	2900	1600	7700	6670	**1584**

Table 4. Statistical comparison of results for the 25-bar truss problem

Algorithm	Best (lb)	Mean (lb)	Worst (lb)	SD (lb)	NFEs
ACO [31]	**484.85**	486.46	N/A	4.71	7700
ABC [41]	**484.85**	484.94	485.05	N/A	24250
HPSO [16]	**484.85**	N/A	N/A	N/A	25000
GA [29]	486.29	N/A	N/A	N/A	N/A
HS [33]	**484.85**	N/A	N/A	N/A	18734
BI [30]	**484.85**	485.76	N/A	1.06	2900
PSO [4]	**484.85**	N/A	N/A	N/A	1600
HS [4]	**484.85**	N/A	N/A	N/A	2100
SA [4]	**484.85**	N/A	N/A	N/A	6624
Ess [4]	485.05	N/A	N/A	N/A	4350
AC [4]	485.05	N/A	N/A	N/A	10050
SGA [4]	485.38	N/A	N/A	N/A	9050
TS [4]	485.57	N/A	N/A	N/A	1626
GAOS [34]	493.8	N/A	N/A	N/A	N/A
HSGA [19]	490.87	N/A	N/A	N/A	2000
BB-BC [32]	**484.85**	485.2	N/A	0.62	6670
CBO [35]	**484.85**	486.87	N/A	N/A	20000
ECBO [35]	**484.85**	485.89	N/A	N/A	20000
WEO [36]	**484.85**	485.252	N/A	N/A	5060
DE [37]	**484.85**	**484.91**	485.38	0.13	< 40000
aeDE [37]	**484.85**	485.01	486.10	0.27	> 15000
FA [38]	**484.85**	485.18	486.29	0.42	< 6000
EFA [38]	**484.85**	485.18	486.82	0.50	> 5000
MBA [39]	**484.85**	484.89	485.05	0.07	25000
DAJA [40]	**484.85**	**484.85**	**484.85**	0.00	25000
HHS [18]	**484.85**	484.946	N/A	0.365	5000
IWOA [43]	**484.85**	484.87	N/A	0.059	15000
oGMO [42]	**484.854**	485.122	N/A	0.223	12000
ESDA	**484.85**	**484.91**	485.05	**0.05**	**5000**

3.2. Example 2: 72-Bar Truss

The second benchmark problem is the 72-bar truss shown in Figure 3. The maximum allowable stress in bars is limited to 25 ksi for both tension and compression. The displacement of the top nodes is restrained to 0.25 inches in both the x and y directions. Using symmetry, all 72 bars are grouped and represented by 16 design variables as follows: (1) A1–A4, (2) A5–A12, (3) A13– A16, (4) A17–A18, (5) A19–A22, (6) A23–A30, (7) A31–A34, (8) A35– A36, (9) A37–A40, (10) A41–A48, (11) A49–A52, (12) A53–A54, (13) A55–A58, (14) A59–A66 (15), A67–A70, and (16) A71–A72. The elasticity modulus of members is set to 10,000 ksi, and material density is specified as 0.1 lb/in^3.

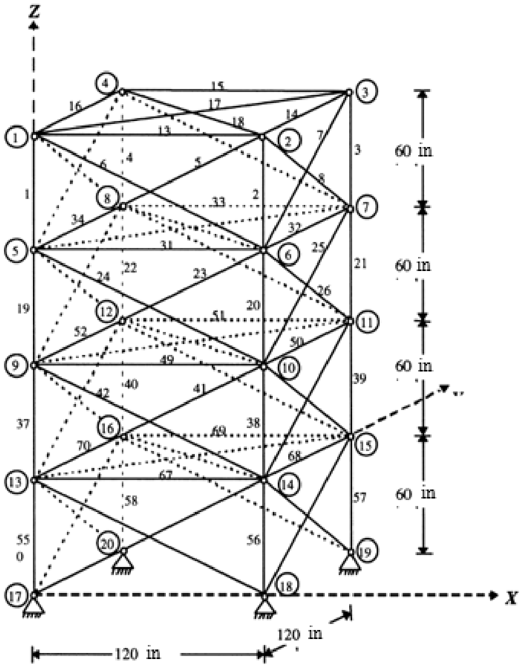

Figure 3. Schematic of the 72-bar truss

The structure is analyzed under two load cases, as summarized in Table 5. For Case 1, design variables are chosen from a predefined set of cross-sections according to AISC-ASD provisions [25]. In Case 2, the cross-sections are treated as continuous variables ranging from 0.1 in^2 to 3.2 in^2.

Table 5. Loads acting on the 72-bar benchmark truss

	Joint	Loads (kips)		
		x	y	z
Case 1	17	5.0	5.0	-5.0
Case 2	17	0.0	0.0	-5.0
	18	0.0	0.0	-5.0
	19	0.0	0.0	-5.0
	20	0.0	0.0	-5.0

Case - 1: Discrete Design Variables

The best designs achieved by ESDA, COA [44], WCA [45], DAJA [40], and DHPSACO [46] are summarized in Table 6. The results show that ESDA reaches the literature-reported optimum of 389.33 lb in only 25 iterations (2,463 analyses), achieving this 25% faster than the previous best benchmark established by DAJA. Additionally, a total of 5,000 analyses were conducted to compare its performance against various metaheuristics, including COA and MCOA [44], WCA, MBA and IMBA [45], ICA [47], DHPSACO, DE and aeDE [37], FA and EFA [38], FWA and IFWA [48], DAJA [40], oGMO [42], SHADE [49], hGMO [50], and ICOOT [51] as reported in Table 7. The comparative results demonstrate the robustness and efficiency of the proposed ESDA in this problem. While several algorithms are able to reach the optimum solution, their mean performance is often degraded due to higher variability across independent runs. When compared to other efficient methods SHADE [49], hGMO [50], and DAJA [40], ESDA remains competitive with offering low computational cost and remarkable consistency. Although a few runs exhibited early convergence, leading to a slightly higher standard deviation than DAJA [40], this has minimal impact on its overall performance. Ultimately, the statistics clearly show that ESDA surpasses all other methods, delivering superior best and mean results with significantly fewer analyses.

Table 6. Comparison of different designs for the 72-bar truss with discrete design variables (Case 1)

Variable Index	Members	COA [44]	WCA [45]	DAJA [40]	ICA [47]	DHPSACO [46]	oGMO [42]	ESDA
1	1-4	1.99	1.99	1.99	1.99	1.8	1.990	**1.99**
2	5-12	0.563	0.442	0.442	0.442	0.442	0.563	**0.442**
3	13-16	0.111	0.111	0.111	0.111	0.141	0.111	**0.111**
4	17,18	0.111	0.111	0.111	0.141	0.111	0.111	**0.111**
5	19-22	1.228	1.228	1.228	1.228	1.228	1.228	**1.228**
6	23-30	0.442	0.563	0.563	0.602	0.563	0.442	**0.563**
7	31-34	0.111	0.111	0.111	0.111	0.111	0.111	**0.111**
8	35,36	0.111	0.111	0.111	0.141	0.111	0.111	**0.111**
9	37-40	0.563	0.563	0.563	0.563	0.563	0.563	**0.563**
10	41-48	0.563	0.563	0.563	0.563	0.563	0.563	**0.563**
11	49-52	0.111	0.111	0.111	0.111	0.111	0.111	**0.111**
12	53,54	0.111	0.111	0.111	0.111	0.25	0.111	**0.111**
13	55-58	0.196	0.196	0.196	0.196	0.196	0.196	**0.196**
14	59-66	0.563	0.563	0.563	0.563	0.563	0.563	**0.563**
15	67-70	0.391	0.391	0.391	0.307	0.442	0.391	**0.391**
16	71,72	0.563	0.563	0.563	0.602	0.563	0.563	**0.563**
	Best (lb)	389.334	389.334	389.334	392.84	393.38	389.33417	**389.3342**
	NFEs (lb)	6800	4600	3376	4500	5330	4100	**2463**

Table 7. Statistical comparison of results for the 72-bar truss problem with discrete design variables (Case 1)

Algorithm	Best (lb)	Mean (lb)	Worst (lb)	SD (lb)	NFEs
COA [44]	**389.334**	393.618	393.965	1.561	8000
MCOA [44]	**389.334**	390.162	392.158	1.018	8000
WCA [45]	**389.334**	389.941	393.778	1.43	50000
MBA [45]	390.739	395.432	399.490	3.04	50000
IMBA [45]	389.334	389.823	N/A	0.84	50000
ICA [47]	392.84	N/A	N/A	N/A	4500
DHPSACO [46]	393.38	N/A	N/A	N/A	5330
DE [37]	**389.334**	390.531	394.170	1.400	> 12000
aeDE [37]	**389.334**	390.913	393.325	1.161	> 4000
FA [38]	**389.334**	391.644	396.245	1.794	> 8000
EFA [38]	**389.334**	391.376	393.826	1.376	> 3000
FWA [48]	394.051	405.03	N/A	N/A	5000
IFWA [48]	**389.334**	389.461	N/A	N/A	5000
DAJA [40]	**389.334**	389.495	**389.828**	**0.159**	>5437
oGMO [42]	389.3342	390.0631	N/A	0.5001	15000
SHADE [49]	389.3342	389.5727	391.3948	0.4458	3990
hGMO [50]	389.334	389.880	N/A	0.267	3950
ICOOT [51]	389.3342	405.1210	453.3486	18.1604	N/A
ESDA	**389.3342**	**389.4369**	390.9522	0.2972	**5000**

Case - 2: Continuous Design Variables

In the continuous design space case of the problem, the number of function evaluations for ESDA is set to 15,000, which is three times greater than that in Case 1. The performance of ESDA is compared against various algorithms, including HBB-BC [17], Multi-Phase BB-BC [32], ACO [31], GA [34], PSO [52], CBO [53], WSA [54], SAHS [55], RO [56], CPA [57], CSP [58], ECBO [59], HTS [60], IGWO [61], TLBO [62], ISRES [63], oGMO [42], ACCS [64], CBSO [65], and dDEmRao-DiC [66]. As shown in Table 8, ESDA slightly improves upon the optimum design reported in the previous studies. Moreover, it produces competitive solutions by improving all statistical metrics from the earlier studies reported in Table 9, except the recent work by Adil & Cengiz [54], which employed the Weighted Superposition Attraction (WSA) algorithm. While ESDA surpasses the best solution reported by WSA using a slightly higher number of function evaluations, its mean result is marginally worse. This may be attributed to two reasons: (i) the number of iterations, which is sufficient for convergence near the optimum since WSA uses only ten samples in its search procedure, and (ii) the tendency of distribution-based algorithms, like ESDA, to exhibit greater variability when fewer samples are used. Consequently, a higher number of function evaluations is necessary to improve the solution. To validate this hypothesis, ESDA was executed again with an increased number of iterations and sample size, set to 150 and 200, respectively. The results revealed that the best and mean results were improved to 379.6151 and 379.6165 lb, respectively, indicating that ESDA can outperform WSA [54] when the sample size is doubled.

Table 8. Comparison of different designs for the 72-bar truss with continuous design variables (Case 2)

Variable Index	Members	GA [34]	PSO [52]	ACO [31]	RO [56]	CPA [57]	oGMO [42]	ESDA
1	1-4	0.161	0.1615	1.948	1.83649	1.8873	1.8515	**1.882518**
2	5-12	0.544	0.5092	0.508	0.502096	0.5111	0.5124	**0.51286**
3	13-16	0.379	0.4967	0.101	0.100007	0.1	0.1000	**0.100001**
4	17,18	0.521	0.5619	0.102	0.10039	0.1	0.1000	**0.100002**
5	19-22	0.535	0.5142	1.303	1.252233	1.2554	1.2436	**1.265879**
6	23-30	0.535	0.5464	0.511	0.503347	0.5141	0.5141	**0.511689**
7	31-34	0.103	0.1	0.101	0.100179	0.1	0.1000	**0.100001**
8	35,36	0.111	0.1095	0.1	0.100151	0.1	0.1000	**0.100000**
9	37-40	1.31	1.3079	0.561	0.572989	0.5312	0.5169	**0.522491**
10	41-48	0.498	0.5193	0.492	0.549872	0.5174	0.5253	**0.516818**
11	49-52	0.11	0.1	0.1	0.100445	0.1	0.1001	**0.100000**
12	53,54	0.103	0.1	0.107	0.100102	0.1	0.1013	**0.100004**
13	55-58	1.91	1.7427	0.156	0.157583	0.1564	0.1561	**0.156411**
14	59-66	0.525	0.5185	0.55	0.52222	0.5443	0.5556	**0.547325**
15	67-70	0.122	0.1	0.39	0.435582	0.4106	0.4012	**0.409439**
16	71,72	0.103	0.1	0.592	0.597158	0.5717	0.5643	**0.569885**
	Best (lb)	383.12	381.91	380.24	380.458	379.62	379.7234	**379.6162**
	NFEs (lb)	N/A	N/A	18500	19084	23580	11750	**15000**

Table 9. Statistical comparison of results for the 72-bar truss problem with continuous design variables (Case 2)

Algorithm	Best (lb)	Mean (lb)	Worst (lb)	SD (lb)	NFEs
HBB-BC [17]	379.66	381.85	N/A	1.201	13200
Multi-Phase BB-BC [32]	379.85	382.08	N/A	1.912	~19621
ACO [31]	380.24	383.16	N/A	3.66	~18500
GA [34]	383.12	N/A	N/A	N/A	N/A
PSO [52]	381.91	N/A	384.62	N/A	8000
CBO [53]	379.6943	379.8961	N/A	0.0791	15600
WSA [54]	379.618	**379.6201**	N/A	**0.0038**	10000
SAHS [55]	380.62	382.42	383.89	1.38	13742
RO [56]	380.458	382.554	N/A	1.221	19084
CPA [57]	379.62	380.83	N/A	0.61	23580
CSP [58]	379.97	381.560	N/A	1.803	10500
ECBO [59]	379.77	380.39	N/A	0.810	20000
HTS [60]	379.73	382.26	N/A	1.94	13166
IGWO [61]	379.7615	380.6811	N/A	0.7315	11960
TLBO [62]	379.63	380.20	380.83	0.41	25000
ISRES [63]	379.98	N/A	N/A	N/A	N/A
oGMO [42]	379.7234	380.5597	N/A	0.4557	15000
ACCS [64]	379.7512	379.81	N/A	0.148	12000
CBSO [65]	379.6585	379.7445	N/A	0.0684	50000
dDEmRao-DiC [66]	379.6506	379.882	380.4806	0.21203	7727
ESDA	**379.6162**	379.6210	**379.646002**	0.0059	**15000**

3.3. Example 3: 117-Bar Cantilever Truss

The steel cantilever truss, consisting of 117 bars and 30 joints, is investigated by Azad & Hasançebi [67] as well as Azad [68, 69]. A schematic of this truss is given in Figure 4. In this problem, the bars are treated as individual elements without member grouping, resulting in 117 design variables, allowing for a comprehensive evaluation of the algorithm's capabilities in large design spaces [67]. The elastic modulus, yield strength, and density of steel are specified as 200 GPa, 248.2 MPa, and 7.85 ton/m^3, respectively. The structure is subjected to multiple loading cases: (i) +15 kN applied in the x-direction, (ii) +15 kN applied in the y-direction, and (iii) +15 kN applied in the z-direction to all unsupported joints, as tabulated in Table 10. The displacement of each joint in all directions is limited to 4 cm, and the maximum allowable stress in the bars is determined by the AISC-LRFD [26] provisions. The sizing variables are selected from a predefined list of pipe sections provided in Table 11.

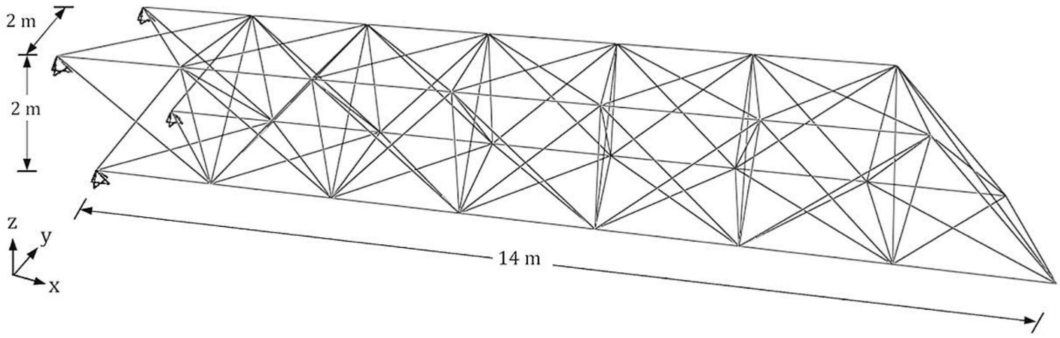

Figure 4. Schematic of the 117-bar cantilever truss

Table 10. Loads acting on the 117-bar cantilever truss

	Joint	Loads (kN)		
		x	y	z
Case 1	All unsupported	15.0	0.0	0.0
Case 2	All unsupported	0.0	15.0	0.0
Case 3	All unsupported	0.0	0.0	15.0

Table 11. Cross-sectional properties of the ready sections from AISC-LRFD [26] provisions

Number	Ready Section	Area (cm^2)	Number	Ready Section	Area (cm^2)	Number	Ready Section	Area (cm^2)
1	PIPE1/2STD	1.6129	14	PIPE3STD	14.3871	26	PIPE5XS	39.4193
2	PIPE1/2XS	2.0645	15	PIPE2-1/2XS	14.5161	27	PIPE4XXS	52.258
3	PIPE3/4STD	2.1484	16	PIPE2XXS	17.1613	28	PIPE6XS	54.1934
4	PIPE3/4XS	2.7935	17	PIPE3-1/2STD	17.2903	29	PIPE8STD	54.1934
5	PIPE1STD	3.1871	18	PIPE3XS	19.4838	30	PIPE5XXS	72.9031
6	PIPE1XS	4.1226	19	PIPE4STD	20.4516	31	PIPE10STD	76.774
7	PIPE1-1/4STD	4.3161	20	PIPE3-1/2XS	23.7419	32	PIPE8XS	82.5805
8	PIPE1-1/2STD	5.1548	21	PIPE2-1/2XXS	25.9999	33	PIPE12STD	94.1934
9	PIPE1-1/4XS	5.6839	22	PIPE5STD	27.7419	34	PIPE6XXS	100.645
10	PIPE1-1/2XS	6.9032	23	PIPE4XS	28.4516	35	PIPE10XS	103.8708
11	PIPE2STD	6.9032	24	PIPE3XXS	35.2903	36	PIPE12XS	123.8707
12	PIPE2XS	9.5484	25	PIPE6STD	35.9999	37	PIPE8XXS	137.4191
13	PIPE2-1/2STD	10.9677						

As mentioned earlier, the sizing optimization of 117-bar truss problems was previously studied using a variety of metaheuristics, including Adaptive Dimensional Search, Big Bang Big Crunch, Guided Stochastic Search, and their enhanced and hybridized versions [67–70]. In the implementation of ESDA, the maximum number of iterations is set to 250, with a population size of 200. As inferred in Table 12, reinforcing the distribution-based Exponential Big Bang–Big Crunch algorithm with convergence-curve monitoring and guided stochastic search heuristics yields a notable enhancement in performance. Nevertheless, owing to its intrinsically balanced distribution-oriented exploration mechanism, ESDA consistently outperforms these reinforced variants as well as other metaheuristics, in terms of both best and mean solutions, and attains the minimum structural weight. A new optimum design of 3,004.62 kg is attained through 50,000 structural analyses, improving the previously reported best design by 31 kg. Additionally, the mean value of the designs obtained from independent runs of ESDA also surpasses the corresponding values reported by the other methods. The best design obtained by ESDA is presented in the supplementary material.

Table 12. Comparison of different designs for the 117-bar steel cantilever truss

Algorithm	Best (kg)	Mean (kg)	Worst (kg)	SD (kg)	NFEs
PSO [67]	3476	3600.7	3828.2	141.1	25000
BB-BC [67]	3586.5	3855.9	4265.5	249.8	25000
EBB-BC [67]	3123.6	3209.9	3277.3	66.8	25000
MBB-BC [67]	3125.4	3205.8	3253.5	60.7	25000
GSS_A [67]	3100.9	3112.3	3133.5	12.6	317
GSS_B [67]	3072.2	3078.3	3085.9	6.6	317
ADS [68]	3078.02	3166.31	3297.07	64.64	50000
EBB-BC [68]	3041.17	3218.80	3692.74	199.30	50000
MBB-BC [68]	3154.90	3298.28	3417.87	90.74	50000
GADS [68]	3067.88	3139.71	3226.14	55.19	50000
GEBB [68]	3035.50	3075.87	3133.86	27.35	50000
GMBB [68]	3058.77	3149.82	3320.91	75.62	50000
GADS_EBB [68]	3047.98	3108.81	3182.31	35.18	50000
GADS_MBB [68]	3069.09	3132.16	3201.15	42.43	50000
GADS_EBB_MBB [68]	3067.46	3128.74	3342.73	82.05	50000
MCC_ADS [69]	3077.79	3127.99	3186.25	28.33	50000
MCC_EB [69]	3041.29	3075.87	3284.28	59.17	50000
MCC_MB [69]	3052.88	3098.57	3286.99	69.92	50000
CSA_M [70]	3628.64	3981.93	4242.35	145.59	150000
ESDA	**3004.62**	**3031.09**	**3051.29**	**13.40**	**50000**

3.4. Example 4: 130-Bar Transmission Tower

The 130-bar transmission tower illustrated schematically in Figure 5, is composed of 33 joints and 130 bars. The cross-sectional areas of the truss members are also selected from a discrete set given in Table 11. The material properties and stress constraints are identical to those used in the 117-bar cantilever steel truss. All nodes are subjected to a displacement constraint of 3 cm in all directions. A single loading case, detailed in Table 13, is applied to the structure.

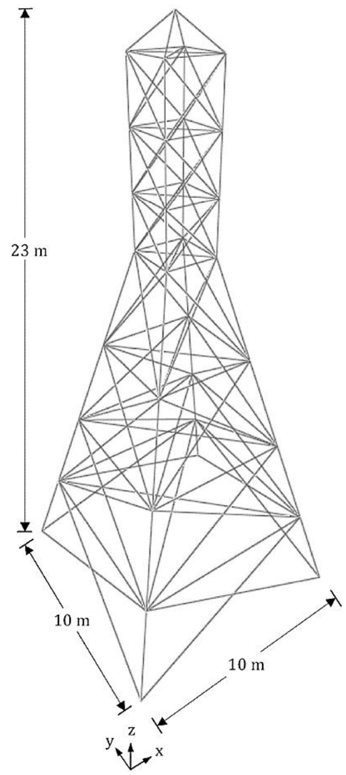

Figure 5. Schematic of the 130-bar transmission tower

Table 13. Loads acting on the 130-bar transmission tower

Joint	Loads (kN)		
	x	y	z
29	100.0	0.0	0.0
30	100.0	0.0	0.0
31	0.0	25.0	0.0
32	0.0	25.0	0.0
33	0.0	0.0	50.0

The problem was previously addressed by Azad et al. [71], where a performance comparison was conducted among the Guided Stochastic Search heuristic, Particle Swarm Optimization, and various versions of Big Bang-Big Crunch algorithms. A summary of this comparison is provided in Table 14. In the implementation of ESDA for this example, the maximum number of iterations is set to 250, with a population size of 200. The results reveal that, similar to the 117-bar cantilever truss problem, ESDA delivers a superior solution, achieving a minimum weight of 5,586.72 kg, with the design details provided in the supplementary material. This outcome corresponds to an improvement of approximately 3.7% over the best design reported in the literature. Moreover, with a standard deviation of only 36.05, ESDA also exhibits the lowest variability, reflecting a level of robustness and reliability not observed in competing methods whose deviations exceed 80–300. Collectively, these results highlight ESDA's capacity to deliver the lightest and most stable designs without incurring additional computational cost.

Table 14. Comparison of different designs for the 130-bar transmission tower

Algorithm	Best (kg)	Mean (kg)	Worst (kg)	SD (kg)	NFEs
PSO [71]	6059.6	6364.3	6611.4	227.3	50000
BB-BC [71]	6427.8	7172.6	6742.9	303.8	50000
EBB-BC [71]	5973.5	6434.7	6144.5	188.9	50000
MBB-BC [71]	5853.9	6526.4	6059.5	240.4	50000
GSS [71]	5801.3	6118.5	6004.4	87.6	50000
ESDA	**5586.72**	**5662.09**	**5760.89**	**36.05**	**50000**

3.5. Example 5: 200-Bar Truss

The 200-bar benchmark truss, schematically illustrated in Figure 6, consists of 77 joints. The truss members are grouped into 29 different sizing variables, which are selected from a discrete set, S = [0.1, 0.347, 0.44, 0.539, 0.954, 1.081, 1.174, 1.333, 1.488, 1.764, 2.142, 2.697, 2.8, 3.131, 3.565, 3.813,4.805, 5.952, 6.572, 7.192, 8.525, 9.3, 10.85, 13.33, 14.29, 17.17, 19.18, 23.68, 28.08, 33.7]. The three load cases applied to the truss are summarized below:

(i) 1.0-kip load is applied to joints 1, 6, 15, 20, 29, 34, 43, 48, 57, 62, 71 in the positive x-direction.

(ii) 10.0-kip load is applied to joints 1, 2, 3, 4, 5, 6, 8, 10, 12, 14, 15, 16, 17, 18, 19, 20, 22, 24, 26, 28, 29, 30, 31, 32, 33, 34, 36, 38, 40, 42, 43, 44, 45, 46, 47, 48, 50, 52, 54, 56, 57, 58, 59, 60, 61, 62, 64, 66, 68, 70, 71, 72, 73, 74, 75 in the negative y-direction.

(iii) Both load cases (i) and (ii) are applied simultaneously.

This problem is governed solely by stress constraints, with the maximum allowable stress set at 10 ksi for both tensile and compressive forces. The material properties include an elastic modulus of 30,000 ksi and a density of 0.283 lb/in^3, respectively.

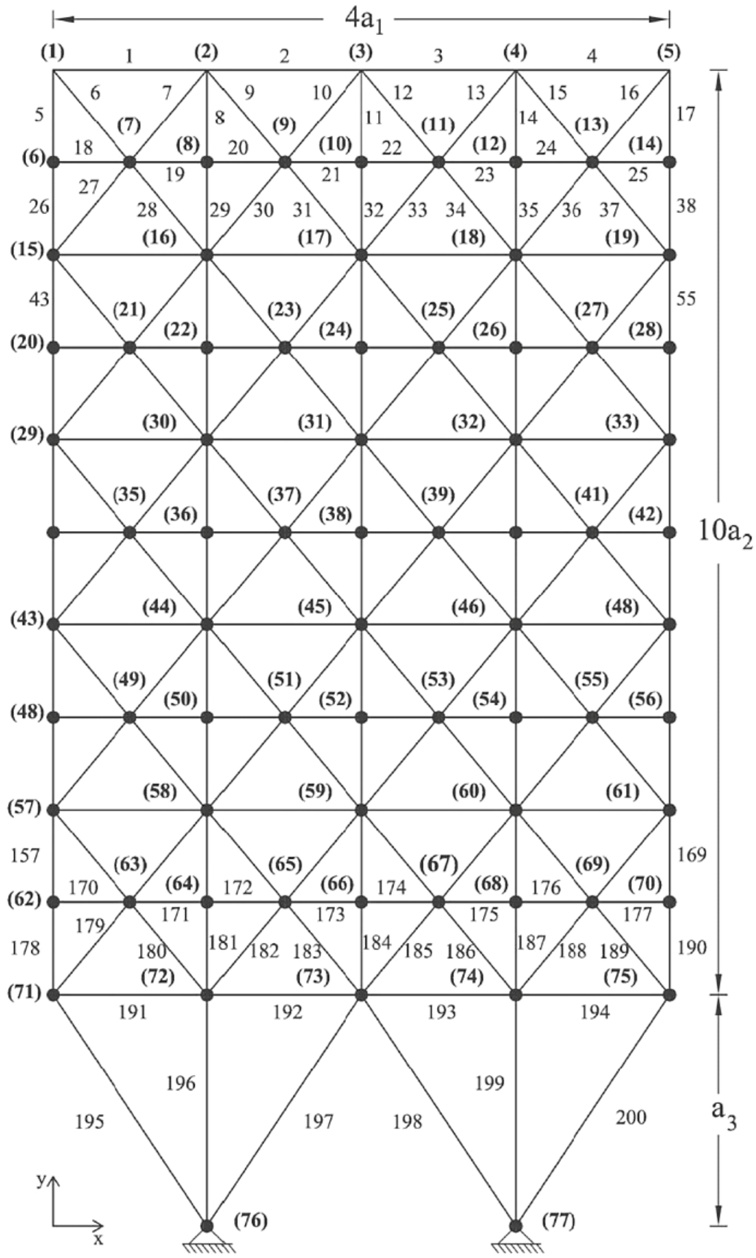

$a_1 = 240$ in. $a_2 = 144$ in. $a_3 = 360$ in

Figure 6. Schematic of the 200-bar truss

The 200-bar truss problem is a widely recognized benchmark example that has been studied using various metaheuristics, including ADS [5], ESASS [72], IGA [73], HACOHS-T [74], FA and EFA [38], DE and aeDE [37], BH, IBH, MV and IMV [75], DAJA [40], and HHS [18]. The best design of the structure attained from 30 independent runs of ESDA is presented alongside the best designs reported by selected algorithms in Table 15, and a full statistical comparison is carried out in Table 16. Accordingly, the best design achieved by ESDA, weighing 27,289.91 lb, is slightly higher than those obtained by HHS [18] and ADS [5], and very close to the results from IMV [75] and DAJA [40], yet it offers a lighter solution than the remaining algorithms. On the other hand, ESDA delivers a lower mean weight with a relatively smaller standard deviation compared to these algorithms, even though this example exhibits greater variability in the optimum designs found, relative to other cases. While HHS [18] and ADS [5] require additional iterations to refine their designs, IMV [75] exhibits significantly greater variability, and DAJA [40] demonstrates limited convergence capability. Overall, although ESDA does not surpass the best design reported to date, it provides a competitive solution by delivering a lower mean weight with reduced variability, achieving superior performance and consistency compared to other algorithms.

Table 15. Comparison of different designs for the 200-bar truss

Variable Index	Members	HHS [18]	ESASS [72]	ADS [5]	ESDA
1	1, 2, 3, 4	0.1	0.1	0.1	**0.1**
2	5, 8, 11, 14, 17	0.954	0.954	0.954	**0.954**
3	19, 20, 21, 22, 23, 24	0.1	0.1	0.347	**0.347**
4	18, 25, 56, 63, 94, 101, 132, 139, 170, 177	0.1	0.1	0.1	**0.1**
5	26, 29, 32, 35, 38	2.142	2.142	2.142	**2.142**
6	6, 7, 9, 10, 12, 13, 15, 16, 27, 28, 30, 31, 33, 34, 36, 37	0.347	0.347	0.347	**0.347**
7	39, 40, 41, 42	0.1	0.1	0.1	**0.1**
8	43, 46, 49, 52, 55	3.131	3.131	3.131	**3.131**
9	57, 58, 59, 60, 61, 62	0.1	0.1	0.1	**0.1**
10	64, 67, 70, 73, 76	4.805	4.805	4.805	**4.805**
11	44, 45, 47, 48, 50, 51, 53, 54, 65, 66, 68, 69, 71, 72, 74, 75	0.44	0.347	0.44	**0.44**
12	77, 78, 79, 80	0.347	0.1	0.1	**0.1**
13	81, 84, 87, 90, 93	5.952	5.952	5.952	**5.952**
14	95, 96, 97, 98, 99, 100	0.347	0.1	0.1	**0.1**
15	102, 105, 108, 111, 114	6.572	6.572	6.572	**6.572**
16	82, 83, 85, 86, 88, 89, 91, 92, 103, 104, 106, 107, 109, 110, 112, 113	0.954	0.44	0.539	**0.539**
17	115, 116, 117, 118	0.347	0.539	0.1	**0.347**
18	119, 122, 125, 128, 131	8.525	7.192	8.525	**8.525**
19	133, 134, 135, 136, 137, 138	0.1	0.44	0.539	**0.347**
20	140, 143, 146, 149, 152	9.3	8.525	9.3	**9.3**
21	120, 121, 123, 124, 126, 127, 129, 130, 141, 142, 144, 145, 147, 148, 150, 151	1.081	0.954	0.954	**0.954**
22	153, 154, 155, 156	0.347	1.174	0.1	**0.954**
23	157, 160, 163, 166, 169	13.33	10.85	10.85	**10.85**
24	171, 172, 173, 174, 175, 176	0.954	0.44	0.954	**0.347**
25	178, 181, 184, 187, 190	13.33	10.85	13.33	**13.33**
26	158, 159, 161, 162, 164, 165, 168, 179, 180, 182, 183, 185, 186, 188, 189	1.764	1.764	1.333	**1.488**
27	191, 192, 193, 194	3.813	8.525	7.192	**6.572**
28	195, 197, 198, 200	8.525	13.33	10.85	**10.85**
29	196, 199	17.17	13.33	14.29	**14.29**
	Weight(lb)	27163.90	28075.49	27190.49	**27289.91**
	Number of structural analyses:	5000	11156	5000	**6255**

Table 16. Statistical comparison of results for the 200-bar benchmark truss

Algorithm	Best (lb)	Mean (lb)	Worst (lb)	SD (lb)	NFEs
ADS [5]	**27190.49**	28146.1	N/A	786.6	5000
ESASS [72]	28075.488	N/A	N/A	N/A	11156
IGA [73]	28544.014	N/A	N/A	N/A	51360
HACOHS-T [74]	28030.20	N/A	N/A	N/A	N/A
FA [38]	28250.570	29871.915	33726.494	481.590	> 20000
EFA [38]	27421.944	28434.603	30180.343	749.0776	> 5000
DE [37]	27901.583	28470.114	29652.891	457.467	45740
aeDE [37]	27858.500	28425.871	29415.000	481.590	11644
FWA [48]	27777.95	29077.12	N/A	708.69	10000
IFWA [48]	27449.25	27859.42	N/A	380.55	10000
BH [75]	30124.50	31375.009	N/A	865.909	15000
IBH [75]	27337.80	28780.12	N/A	745.376	15000
MV [75]	29093.50	31140.377	N/A	1077.402	15000
IMV [75]	27281.35	28771.426	N/A	624.026	15000
DAJA [40]	27282.57	27878.27	**28108.61**	282.88	> 10,783
HHS [18]	**27163.59**	28159.59	N/A	1149.91	5000
ESDA	27289.909	**27833.746**	28423.663	**267.2697**	10000

3.6. Example 6: 354-Bar Dome Truss

The 354-bar steel dome truss is illustrated schematically in Figure 7. In this example, the bars are treated as individual elements without grouping, resulting in 354 design variables. Material properties, stress constraints, and the section list are identical to those used in the 117-bar cantilever truss and 130-bar transmission tower. The displacement of the dome tip is limited to 2 cm. All unsupported joints are subjected to a 15 kN load in the negative z-direction, and an additional 100 kN load is applied to the topmost joint in the same direction.

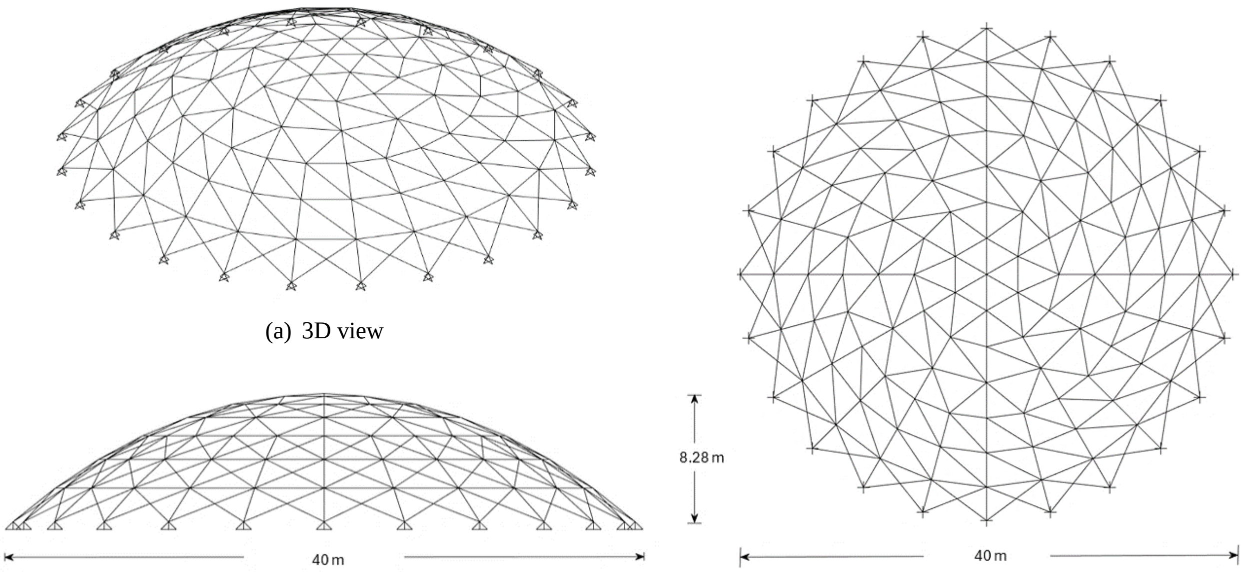

(a) 3D view

(b) side view

(c) top view

Figure 7. Schematics of the 354-bar dome truss, (a) 3D view, (b) side view, and (c) top view

This problem was previously investigated by Azad [68]. ESDA was implemented for this example with a population size of 500 samples over 400 iterations. The findings in Table 17 offer clear evidence of the advantages of ESDA over both classical and recently proposed metaheuristics. Despite being tested under the same computational budget of 200,000 NFEs, competing methods such as ADS, GEBB, and GADS [68] could only achieve best solutions between 13,614 and 13,967 kg, with average results typically above 14,000 kg and worst outcomes often exceeding 15,000 kg. Even hybrid variants, including GADS_EBB and GADS_MBB [68], provided no tangible improvement and in fact introduced considerable variability, as reflected in standard deviations well above 500 kg. ESDA, by contrast, consistently delivered superior solutions: its best design of 13,471.86 kg improves upon the nearest competitor (GADS [68]) by more than 140 kg, while its mean value (13,694.00 kg) and worst-case result (13,841.05 kg) remain lower than the best solutions of all other algorithms. Importantly, ESDA achieved this with an exceptionally small standard deviation of just 89.13, highlighting its ability to reproduce high-quality results reliably across independent trials. In practical terms, these results illustrate that ESDA not only finds lighter designs but also does so with far greater stability and predictability than its peers, which makes it a compelling framework for tackling larger-scale and complex structural optimization problems.

Table 17. Statistical comparison of results for the 354-bar truss dome

Algorithm	Best (kg)	Mean (kg)	Worst (kg)	SD (kg)	NFEs
ADS [68]	13945.55	14469.43	15072.98	339.01	200000
EBB-BC [68]	14021.88	14715.87	16059.02	561.71	200000
MBB-BC [68]	15279.94	16057.03	17137.68	580.64	200000
GADS [68]	13614.55	14064.70	14702.13	337.08	200000
GEBB [68]	13966.80	14426.17	14871.37	298.6	200000
GMBB [68]	14672.29	16929.17	19595.92	1601.22	200000
GADS_EBB [68]	13653.34	14249.88	15358.57	534.79	200000
GADS_MBB [68]	13954.33	14774.50	16227.15	776.90	200000
GADS_EBB_MBB [68]	13780.96	14712.15	15926.40	632.00	200000
ESDA	**13471.86**	**13694.00**	**13841.05**	**89.13**	**200000**

3.7. Example 7: 942-Bar Tower Truss

The last design example in this study is the 26-story, 942-bar tower truss. As shown in Figure 8, the tower consists of three sections, with a total of 59 member groups. These groups have continuous sizing variables ranging from 0.1 to 200 in^2. The elastic modulus and material density for this problem are 10,000 ksi and 0.1 lb/in^2, respectively. The bars are subjected to a maximum allowable stress of 25 ksi in both tension and compression, and the displacement of the topmost four joints is limited to 15 inches in the x, y and z directions. The tower is symmetric around the x and y axes. The loads applied in the x, y, and z directions are summarized as follows:

- **(i)** In the x-direction: +1.5 kips on the nodes located on the left side (including the center nodes) and +1.0 kip on the right side;
- **(ii)** In the y-direction: +1.0 kip for all nodes;
- **(iii)** In the z-direction: -3.0, -6.0, and -9.0 kips on the nodes located in the first, second, and third sections, respectively.

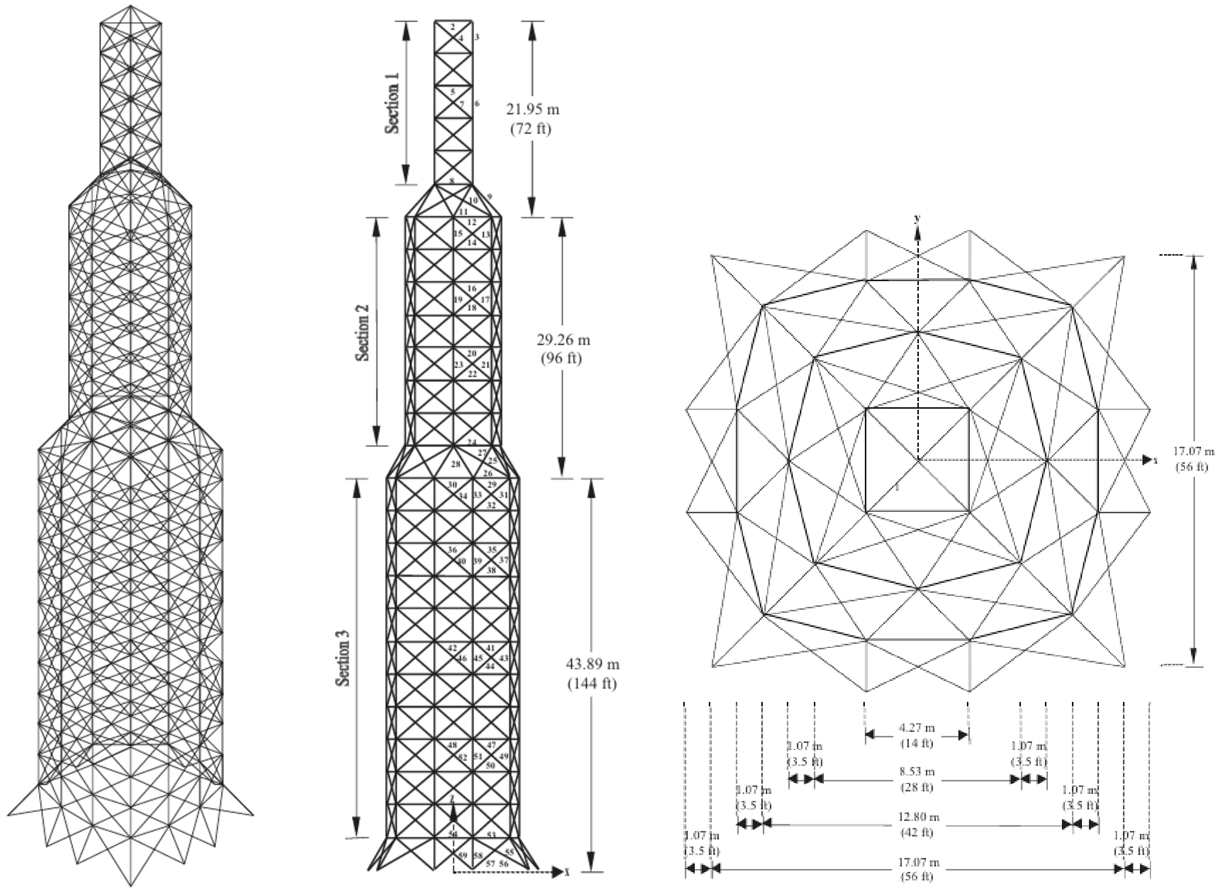

(a) 3D view **(b) side view** **(c) top view**

Figure 8. Schematic of the 942-bar tower truss, (a) 3D view, (b) side view, and (c) top view

Ambiguity in the description of the x-direction loads on the central nodes (x = 0) has resulted in varying treatments of this problem in the literature, yet prior studies have compared optimum solutions without properly accounting for these differences. To ensure a fair comparison, the reported optimum designs were reanalyzed using our structural analysis code and only results corresponding to the specified load case are presented.

This problem has been previously studied using several algorithms, including AES [76], SA [77], JAYA [24], GNMS [78], FFA [79], and MAISA [80]. ESDA was implemented for this example with a population size of 400 samples over 250 iterations. The reported best designs and statistical comparison of the solutions produced by various algorithms are presented in Tables 18 and 19, respectively. Although Gandomi et al. [81] reported an optimum result of 134,119.6 lb, the problem was somewhat modified since the center joint (x=0) was subjected to a load of +1.0 kip, rather than +1.5 kips as considered in this study. Among the six feasible results reported in the tables, the designs produced by ESDA and JAYA [24] are the most competitive. JAYA shows evolutionary behavior, in which a higher number of iterations is performed using a lower population size, whereas ESDA implements a higher number of structural analyses to ensure convergence to the best available design. The results show that ESDA improves upon the best design of JAYA by more than 120 lb. ESDA was also able to reach JAYA's best solution in 113 iterations, indicating faster convergence compared to JAYA. While ESDA slightly enhances the mean result achieved by JAYA, it exhibits a marginally higher standard deviation due to the inherent characteristics of distribution-based algorithms.

Table 18. Comparison of different designs for the 942-bar tower truss problem

Variable Index	SA [77]	GNMS [78]	AES [76]	JAYA [24]	ESDA
1	1	2.7859	1.02	1.045258	**1.004178**
2	1	1.3572	1.037	1.00163	**1.000709**
3	3	5.0362	2.943	3.549999	**3.246822**
4	1	2.2398	1.92	1.92459	**1.835223**
5	1	1.2226	1.025	1.000032	**1.000863**
6	17	14.9575	14.961	15.33708	**14.966988**
7	3	2.9568	3.074	3.108905	**3.071568**
8	7	10.9038	6.78	6.589077	**6.945463**
9	20	14.4177	18.58	16.56966	**17.292298**
10	1	3.7090	2.415	2.553777	**2.703624**
11	8	5.7076	6.584	6.433946	**6.099534**
12	7	4.9264	6.291	5.812166	**5.675526**
13	19	14.1751	15.383	15.83688	**15.490186**
14	2	1.9043	2.1	2.196943	**2.233097**
15	5	2.8101	6.021	4.324553	**4.317106**
16	1	1.0000	1.022	1.000047	**1.000823**
17	22	18.8070	23.099	21.97377	**21.995683**
18	3	2.6151	2.889	2.674909	**2.704847**
19	9	12.5328	7.96	8.722646	**8.302610**
20	1	1.1314	1.008	1.000032	**1.000700**
21	34	30.5122	28.548	29.89861	**29.400846**
22	3	3.3460	3.349	3.249223	**3.319940**
23	19	17.0450	16.144	16.99562	**16.477752**
24	27	18.0785	24.822	25.51041	**25.187918**
25	42	39.2717	38.401	37.63407	**37.336824**
26	1	2.6062	3.787	1.220731	**1.616201**
27	12	9.8303	12.32	11.94408	**11.823109**
28	16	13.1126	17.036	16.515	**16.451946**
29	19	13.6897	14.733	14.82289	**14.539647**
30	14	16.9776	15.031	15.98357	**15.717375**
31	42	37.6006	38.597	38.51425	**38.247991**
32	4	3.0602	3.511	3.323571	**3.279045**
33	4	5.5106	2.997	3.189674	**3.212573**
34	4	1.8014	3.06	2.82237	**2.707864**
35	1	1.1568	1.086	1.001323	**1.000178**
36	1	1.2423	1.462	1.002606	**1.000657**
37	62	62.7741	59.433	59.53012	**59.054679**
38	3	3.3276	3.632	3.250054	**3.293982**
39	2	4.2369	1.887	2.068093	**1.871094**
40	4	1.7202	4.072	3.084539	**3.193299**
41	1	1.0148	1.595	1.000717	**1.000245**
42	2	5.4628	3.671	1.239938	**1.935353**
43	77	78.0094	79.511	79.89118	**79.706585**
44	3	3.2206	3.394	3.299488	**3.286241**
45	2	3.5934	1.581	1.964128	**1.713053**
46	3	4.7668	4.204	3.489718	**3.481911**
47	2	1.1531	1.329	1.000032	**1.001021**
48	3	2.1698	2.242	1.000032	**1.001372**
49	100	99.6406	96.886	97.18147	**95.707246**
50	4	4.1469	3.71	3.322281	**3.377505**
51	1	2.1600	1.055	1.002997	**1.574221**
52	4	4.1499	4.566	3.651629	**3.787710**
53	6	11.2070	9.606	7.226228	**9.454469**
54	3	11.0904	2.984	4.544599	**7.083401**
55	49	35.9499	45.917	41.41107	**42.491303**
56	1	2.1937	1	1.002207	**1.000471**
57	62	66.1705	62.426	64.80352	**62.769092**
58	1	3.3402	2.977	2.525618	**3.873196**
59	3	4.0525	1	1.000054	**1.034346**
Weight(lb)	143436	142295.8	141241	137344.356	**137222.24**
Number of structural analyses:	39834	N/A	150000	58274	**99801**

Table 19. Statistical comparison of results for the 942-bar tower truss problem

Algorithm	Best (lb)	Mean (lb)	Worst (lb)	SD (lb)	NFEs
AES [76]	141241	N/A	N/A	N/A	150000
SA [77]	143436.02	N/A	N/A	N/A	N/A
JAYA [24]	137344.356	137379.616	137420.440	38.346	~70000
GNMS [78]	142295.75	N/A	N/A	N/A	N/A
FFA [79]	138878	139682	142265	1098	50000
MAISA [80]	142287.47	142994.38	N/A	641.27	217500
ESDA	**137222.24**	**137356.60**	**137581.43**	**91.13**	**100000**

4. Conclusion

In the present study, the Elitist Stepped Distribution Algorithm (ESDA), a recently developed distribution-based metaheuristic, is introduced, implemented, and rigorously evaluated for truss sizing optimization problems, marking its first application in the structural optimization literature. The performance of ESDA in structural optimization was investigated through a series of test problems: (i) 25-bar truss, (ii) 72-bar truss, (iii) 117-bar cantilever truss, (iv) 130-bar transmission tower, (v) 200-bar truss, (vi) 354-bar dome truss, and (vii) 942-bar tower truss. These examples were specifically selected to cover a broad spectrum of problem characteristics, including (i) both discrete and continuous solution sets, (ii) grouped and ungrouped design variables, and (iii) single and multiple loading cases with both displacement and stress constraints. This diverse selection of problems was intended to simulate real-world structural design challenges, providing a robust evaluation of ESDA's effectiveness across a wide range of optimization scenarios.

ESDA demonstrated a strong performance by achieving the previously reported optimum design weights for the 25-bar and 72-bar benchmark trusses with fewer structural analyses and lower standard deviations compared to most metaheuristics in the literature. Similarly, for the 200-bar benchmark truss, ESDA achieved the best mean weight and standard deviation across 30 independent runs. The algorithm further demonstrated its efficacy on complex problems with a large number of design variables, such as the 117-bar cantilever truss, 130-bar transmission tower, and 354-bar dome truss, where it improved upon previously reported results. One-sided Welch's t-tests with 95% confidence intervals confirmed that ESDA achieved significantly lower mean weights than the compared algorithms on these benchmarks, with all confidence intervals lying entirely in the negative domain. Notably, for the 942-bar tower truss design problem involving numerous bars and grouped design variables, ESDA set a new optimum design, surpassing the best existing solution. However, the statistical test indicates that the improvement over the literature-reported best performance of JAYA was not statistically significant.

The solutions produced by ESDA underscore the algorithm's robustness and efficiency in truss sizing optimization problems. Notably, as the number of design variables and the complexity of the solution set grow, ESDA has shown a distinct advantage in enhancing solution quality compared to other metaheuristics applied to similar problems. Unlike evolutionary algorithms, which heavily depend on numerous iterations to achieve optimal results, ESDA benefits from a larger sample size within a moderate number of iterations as the problem's complexity increases. This approach enhances the algorithm's exploration capability, enabling a more thorough search across the solution space. Nonetheless, scaling ESDA to problems involving thousands of design variables and highly nonlinear constraints may present challenges, particularly in terms of sampling efficiency, constraint-handling, and computational cost. Addressing these aspects through adaptive sampling strategies, hybridization with local search, and adaptive or multi-objective mechanisms could enhance its applicability to such large-scale settings. Taken together, these outcomes highlight ESDA's scalability while also indicating promising avenues, including its extension to truss layout and topology optimization, as well as to alternative structural systems such as frames and shells, which would further broaden its utility in structural design optimization.

5. Declarations

5.1. Author Contributions

Conceptualization, M.A. and O.P.; methodology, M.T. and M.A.; software, M.T.; validation, M.T. and M.A.; formal analysis, M.T. and M.A.; investigation, M.T.; data curation, O.H.; writing—original draft preparation, M.T. and M.A.; writing—review and editing, M.A., O.P., and O.H.; visualization, M.T.; supervision, O.P. and O.H. All authors have read and agreed to the published version of the manuscript.

5.2. Data Availability Statement

The data presented in this study are available on request from the corresponding author.

5.3. Funding

The authors received no financial support for the research, authorship, and/or publication of this article.

5.4. Conflicts of Interest

The authors declare no conflict of interest.

6. References

[1] Pucker, T., & Grabe, J. (2011). Structural optimization in geotechnical engineering: Basics and application. Acta Geotechnica, 6(1), 41–49. doi:10.1007/s11440-011-0134-7.

[2] Keleşoğlu, Ö., & Ülker, M. (2005). Fuzzy optimization of geometrical nonlinear space truss design. Turkish Journal of Engineering and Environmental Sciences, 29(5), 321–329.

[3] Stolpe, M. (2016). Truss optimization with discrete design variables: a critical review. Structural and Multidisciplinary Optimization, 53(2), 349–374. doi:10.1007/s00158-015-1333-x.

[4] Hasançebi, O., Çarbaş, S., Doğan, E., Erdal, F., & Saka, M. P. (2009). Performance evaluation of metaheuristic search techniques in the optimum design of real size pin jointed structures. Computers and Structures, 87(5–6), 284–302. doi:10.1016/j.compstruc.2009.01.002.

[5] Hasançebi, O., & Azad, S. K. (2015). Adaptive dimensional search: A new metaheuristic algorithm for discrete truss sizing optimization. Computers and Structures, 154, 1–16. doi:10.1016/j.compstruc.2015.03.014.

[6] Whitley, D. (1994). A genetic algorithm tutorial. Statistics and Computing, 4(2), 65–85. doi:10.1007/BF00175354.

[7] Storn, R., & Price, K. (1997). Differential Evolution - A Simple and Efficient Heuristic for Global Optimization over Continuous Spaces. Journal of Global Optimization, 11(4), 341–359. doi:10.1023/A:1008202821328.

[8] Kennedy, J., & Eberhart, R. (n.d.). Particle swarm optimization. Proceedings of ICNN'95 - International Conference on Neural Networks, 4, 1942–1948. doi:10.1109/icnn.1995.488968.

[9] Dorigo, M., & Di Caro, G. (1999). Ant colony optimization: a new meta-heuristic. Proceedings of the 1999 Congress on Evolutionary Computation-CEC99 (Cat. No. 99TH8406), 1470–1477. doi:10.1109/cec.1999.782657.

[10] Kirkpatrick, S., Gelatt, C. D., & Vecchi, M. P. (1983). Optimization by simulated annealing. Science, 220(4598), 671–680. doi:10.1126/science.220.4598.671.

[11] Altun, M., & Pekcan, O. (2021). Optimum Sizing of Truss Structures Using a Hybrid Flower Pollinations. Applications of Flower Pollination Algorithm and its Variants. Springer Tracts in Nature-Inspired Computing. Springer, Singapore. doi:10.1007/978-981-33-6104-1_6.

[12] Erol, O. K., & Eksin, I. (2006). A new optimization method: Big Bang-Big Crunch. Advances in Engineering Software, 37(2), 106–111. doi:10.1016/j.advengsoft.2005.04.005.

[13] Yalcin, Y., Orhon, M., & Pekcan, O. (2019). An automated approach for the design of Mechanically Stabilized Earth Walls incorporating metaheuristic optimization algorithms. Applied Soft Computing, 74, 547–566. doi:10.1016/j.asoc.2018.09.039.

[14] Mirjalili, S., Mirjalili, S. M., & Lewis, A. (2014). Grey Wolf Optimizer. Advances in Engineering Software, 69, 46–61. doi:10.1016/j.advengsoft.2013.12.007.

[15] Gandomi, A. H., Yang, X. S., & Alavi, A. H. (2013). Cuckoo search algorithm: A metaheuristic approach to solve structural optimization problems. Engineering with Computers, 29(1), 17–35. doi:10.1007/s00366-011-0241-y.

[16] Li, L. J., Huang, Z. B., & Liu, F. (2009). A heuristic particle swarm optimization method for truss structures with discrete variables. Computers and Structures, 87(7–8), 435–443. doi:10.1016/j.compstruc.2009.01.004.

[17] Kaveh, A., & Talatahari, S. (2009). Size optimization of space trusses using Big Bang-Big Crunch algorithm. Computers and Structures, 87(17–18), 1129–1140. doi:10.1016/j.compstruc.2009.04.011.

[18] Cheng, M. Y., Prayogo, D., Wu, Y. W., & Lukito, M. M. (2016). A Hybrid Harmony Search algorithm for discrete sizing optimization of truss structure. Automation in Construction, 69, 21–33. doi:10.1016/j.autcon.2016.05.023.

[19] Ponterosso, P., & Fox, D. S. J. (1999). Heuristically seeded genetic algorithms applied to truss optimisation. Engineering with Computers, 15(4), 345–355. doi:10.1007/s003660050029.

[20] Kaveh, A., & Talatahari, S. (2009). Particle swarm optimizer, ant colony strategy and harmony search scheme hybridized for optimization of truss structures. Computers & Structures, 87(5–6), 267–283. doi:10.1016/j.compstruc.2009.01.003.

[21] Tutuş, E.B., Pekcan, O., Altun, M., & Türkezer, M. (2021). Optimizing Reinforced Cantilever Retaining Walls Under Dynamic Loading Using Improved Flower Pollination Algorithm. Applications of Flower Pollination Algorithm and its Variants. Springer Tracts in Nature-Inspired Computing. Springer, Singapore. doi:10.1007/978-981-33-6104-1_7.

[22] Rubinstein, R. (1999). The Cross-Entropy Method for Combinatorial and Continuous Optimization. In Methodology And Computing In Applied Probability (Vol. 1, Issue 2, pp. 127–190). doi:10.1023/a:1010091220143.

[23] Rajeev, S., & Krishnamoorthy, C. S. (1992). Discrete Optimization of Structures Using Genetic Algorithms. Journal of Structural Engineering, 118(5), 1233–1250. doi:10.1061/(asce)0733-9445(1992)118:5(1233).

[24] Degertekin, S. O., Lamberti, L., & Ugur, I. B. (2018). Sizing, layout and topology design optimization of truss structures using the Jaya algorithm. Applied Soft Computing Journal, 70, 903–928. doi:10.1016/j.asoc.2017.10.001.

[25] AISC. (2016). Specification for Structural Steel Buildings-Allowable Stress Design and Plastic Design. American Institute of Steel Construction (AISC), Chicago, United States.

[26] AISC. (1994). Manual of Steel Construction, Load & Resistance Factor Design. American Institute of Steel Construction (AISC), Chicago, United States.

[27] Altun, M., & Pekcan, O. (2017). A modified approach to cross entropy method: Elitist stepped distribution algorithm. Applied Soft Computing Journal, 58, 756–769. doi:10.1016/j.asoc.2017.04.032.

[28] Hasançebi, O., Çarbas, S., & Saka, M. P. (2011). A reformulation of the ant colony optimization algorithm for large scale structural optimization. Civil-Comp Proceedings, 97. doi:10.4203/ccp.97.12.

[29] Wu, S. J., & Chow, P. T. (1995). Steady-state genetic algorithms for discrete optimization of trusses. Computers & Structures, 56(6), 979–991. doi:10.1016/0045-7949(94)00551-D.

[30] Hasançebi, O., Teke, T., & Pekcan, O. (2013). A bat-inspired algorithm for structural optimization. Computers and Structures, 128, 77–90. doi:10.1016/j.compstruc.2013.07.006.

[31] Camp, C. V., & Bichon, B. J. (2004). Design of Space Trusses Using Ant Colony Optimization. Journal of Structural Engineering, 130(5), 741–751. doi:10.1061/(asce)0733-9445(2004)130:5(741).

[32] Camp, C. V. (2007). Design of Space Trusses Using Big Bang–Big Crunch Optimization. Journal of Structural Engineering, 133(7), 999–1008. doi:10.1061/(asce)0733-9445(2007)133:7(999).

[33] Lee, K. S., Geem, Z. W., Lee, S. H. O., & Bae, K. W. (2005). The harmony search heuristic algorithm for discrete structural optimization. Engineering Optimization, 37(7), 663–684. doi:10.1080/03052150500211895.

[34] Erbatur, F., Hasançebi, O., Tütüncü, İ., & Kılıç, H. (2000). Optimal design of planar and space structures with genetic algorithms. Computers and Structures, 75(2), 209–224. doi:10.1016/S0045-7949(99)00084-X.

[35] Kaveh, A., & Ilchi Ghazaan, M. (2015). A comparative study of CBO and ECBO for optimal design of skeletal structures. Computers & Structures, 153, 137–147. doi:10.1016/j.compstruc.2015.02.028.

[36] Kaveh, A., & Bakhshpoori, T. (2016). An accelerated water evaporation optimization formulation for discrete optimization of skeletal structures. Computers & Structures, 177, 218–228. doi:10.1016/j.compstruc.2016.08.006.

[37] Ho-Huu, V., Nguyen-Thoi, T., Vo-Duy, T., & Nguyen-Trang, T. (2016). An adaptive elitist differential evolution for optimization of truss structures with discrete design variables. Computers & Structures, 165, 59–75. doi:10.1016/j.compstruc.2015.11.014.

[38] Le, D. T., Bui, D. K., Ngo, T. D., Nguyen, Q. H., & Nguyen-Xuan, H. (2019). A novel hybrid method combining electromagnetism-like mechanism and firefly algorithms for constrained design optimization of discrete truss structures. Computers & Structures, 212, 20–42. doi:10.1016/j.compstruc.2018.10.017.

[39] Sadollah, A., Bahreininejad, A., Eskandar, H., & Hamdi, M. (2012). Mine blast algorithm for optimization of truss structures with discrete variables. Computers & Structures, 102–103, 49–63. doi:10.1016/j.compstruc.2012.03.013.

[40] Degertekin, S. O., Lamberti, L., & Ugur, I. B. (2019). Discrete sizing/layout/topology optimization of truss structures with an advanced Jaya algorithm. Applied Soft Computing Journal, 79, 363–390. doi:10.1016/j.asoc.2019.03.058.

[41] Sonmez, M. (2011). Discrete optimum design of truss structures using artificial bee colony algorithm. Structural and Multidisciplinary Optimization, 43(1), 85–97. doi:10.1007/s00158-010-0551-5.

[42] Pham, V. H. S., Nguyen Dang, N. T., & Nguyen, V. N. (2024). Achieving efficiency in truss structural design using opposition-based geometric mean optimizer. Soft Computing, 28(17–18), 9883–9903. doi:10.1007/s00500-024-09838-1.

[43] Jiang, F., Wang, L., & Bai, L. (2021). An Improved Whale Algorithm and Its Application in Truss Optimization. Journal of Bionic Engineering, 18(3), 721–732. doi:10.1007/s42235-021-0041-z.

[44] Pierezan, J., dos Santos Coelho, L., Cocco Mariani, V., Hochsteiner de Vasconcelos Segundo, E., & Prayogo, D. (2021). Chaotic coyote algorithm applied to truss optimization problems. Computers and Structures, 242, 106353–106353. doi:10.1016/j.compstruc.2020.106353.

[45] Sadollah, A., Eskandar, H., Bahreininejad, A., & Kim, J. H. (2015). Water cycle, mine blast and improved mine blast algorithms for discrete sizing optimization of truss structures. Computers & Structures, 149, 1–16. doi:10.1016/j.compstruc.2014.12.003.

[46] Kaveh, A., & Talatahari, S. (2009). A particle swarm ant colony optimization for truss structures with discrete variables. Journal of Constructional Steel Research, 65(8–9), 1558–1568. doi:10.1016/j.jcsr.2009.04.021.

[47] Kaveh, A., & Talatahari, S. (2010). Optimum design of skeletal structures using imperialist competitive algorithm. Computers & Structures, 88(21–22), 1220–1229. doi:10.1016/j.compstruc.2010.06.011.

[48] Gholizadeh, S., & Milany, A. (2018). An improved fireworks algorithm for discrete sizing optimization of steel skeletal structures. Engineering Optimization, 50(11), 1829–1849. doi:10.1080/0305215X.2017.1417402.

[49] Kaveh, A., & Biabani Hamedani, K. (2025). Success-History Based Adaptive Differential Evolution Algorithm for Discrete Structural Optimization. Iranian Journal of Science and Technology - Transactions of Civil Engineering, 49(1), 409–431. doi:10.1007/s40996-024-01490-x.

[50] Pham, V. H. S., Nguyen Dang, N. T., & Nguyen, V. N. (2024). Efficient Truss Design: A Hybrid Geometric Mean Optimizer for Better Performance. Applied Computational Intelligence and Soft Computing, 2024(4216718). doi:10.1155/2024/4216718.

[51] Fardi Zarnagh, S., Nouri, M., & Mousavi Ghasemi, S. A. (2026). Optimum Design of Larg Scale Truss Structuree by Levy Flight-Based Improved Coot Optimization Algorithm Considering Discrete Variables. International Journal of Engineering, Transactions B: Applications, 39(1), 59–75. doi:10.5829/ije.2026.39.01a.06.

[52] Perez, R. E., & Behdinan, K. (2007). Particle swarm approach for structural design optimization. Computers & Structures, 85(19–20), 1579–1588. doi:10.1016/j.compstruc.2006.10.013.

[53] Kaveh, A., & Mahdavi, V. R. (2014). Colliding bodies optimization: A novel meta-heuristic method. Computers and Structures, 139, 18–27. doi:10.1016/j.compstruc.2014.04.005.

[54] Adil, B., & Cengiz, B. (2020). Optimal design of truss structures using weighted superposition attraction algorithm. Engineering with Computers, 36(3), 965–979. doi:10.1007/s00366-019-00744-x.

[55] Degertekin, S. O. (2012). Improved harmony search algorithms for sizing optimization of truss structures. Computers & Structures, 92–93, 229–241. doi:10.1016/j.compstruc.2011.10.022.

[56] Kaveh, A., & Khayatazad, M. (2013). Ray optimization for size and shape optimization of truss structures. Computers & Structures, 117, 82–94. doi:10.1016/j.compstruc.2012.12.010.

[57] Kaveh, A., & Zolghadr, A. (2017). Cyclical parthenogenesis algorithm for layout optimization of truss structures with frequency constraints. Engineering Optimization, 49(8), 1317-1334. doi:10.1080/0305215X.2016.1245730.

[58] Kaveh, A., Sheikholeslami, R., Talatahari, S., & Keshvari-Ilkhichi, M. (2014). Chaotic swarming of particles: A new method for size optimization of truss structures. Advances in Engineering Software, 67, 136–147. doi:10.1016/j.advengsoft.2013.09.006.

[59] Kaveh, A., & Ilchi Ghazaan, M. (2014). Enhanced colliding bodies optimization for design problems with continuous and discrete variables. Advances in Engineering Software, 77, 66–75. doi:10.1016/j.advengsoft.2014.08.003.

[60] Degertekin, S. O., Lamberti, L., & Hayalioglu, M. S. (2017). Heat transfer search algorithm for sizing optimization of truss structures. Latin American Journal of Solids and Structures, 14(3), 373–397. doi:10.1590/1679-78253297.

[61] Kaveh, A., & Zakian, P. (2018). Improved GWO algorithm for optimal design of truss structures. Engineering with Computers, 34(4), 685–707. doi:10.1007/s00366-017-0567-1.

[62] Degertekin, S. O., & Hayalioglu, M. S. (2013). Sizing truss structures using teaching-learning-based optimization. Computers and Structures, 119, 177–188. doi:10.1016/j.compstruc.2012.12.011.

[63] Avcı, M. S., Yavuz, D., Ercan, E., & Nuhoğlu, A. (2024). Efficient Sizing and Layout Optimization of Truss Benchmark Structures Using ISRES Algorithm. Applied Sciences (Switzerland), 14(8), 3324. doi:10.3390/app14083324.

[64] Kooshkbaghi, M., & Kaveh, A. (2020). Sizing Optimization of Truss Structures with Continuous Variables by Artificial Coronary Circulation System Algorithm. Iranian Journal of Science and Technology - Transactions of Civil Engineering, 44(1), 1–20. doi:10.1007/s40996-019-00254-2.

[65] Nemati, M., Zandi, Y., & Sabouri, J. (2024). Truss sizing optimum design using a metaheuristic approach: Connected banking system. Heliyon, 10(20), e39308. doi:10.1016/j.heliyon.2024.e39308.

[66] Pham, H. A., & Vu, T. C. (2024). Enhanced differential evolution-Rao optimization with distance comparison method and its application in optimal sizing of truss structures. Journal of Computational Science, 80, 102327. doi:10.1016/j.jocs.2024.102327.

[67] Azad, S. K., & Hasançebi, O. (2015). Discrete sizing optimization of steel trusses under multiple displacement constraints and load cases using guided stochastic search technique. Structural and Multidisciplinary Optimization, 52(2), 383–404. doi:10.1007/s00158-015-1233-0.

[68] Azad, S. K. (2017). Enhanced hybrid metaheuristic algorithms for optimal sizing of steel truss structures with numerous discrete variables. Structural and Multidisciplinary Optimization, 55(6), 2159–2180. doi:10.1007/s00158-016-1634-8.

[69] Azad, S. K. (2019). Monitored convergence curve: a new framework for metaheuristic structural optimization algorithms. Structural and Multidisciplinary Optimization, 60(2), 481–499. doi:10.1007/s00158-019-02219-5.

[70] Ozbasaran, H., & Eryilmaz Yildirim, M. (2020). Truss-sizing optimization attempts with CSA: a detailed evaluation. Soft Computing, 24(22), 16775–16801. doi:10.1007/s00500-020-04972-y.

[71] Azad, S., Hasançebi, O., & Saka, M. P. (2014). Guided stochastic search technique for discrete sizing optimization of steel trusses: A design-driven heuristic approach. Computers and Structures, 134, 62–74. doi:10.1016/j.compstruc.2014.01.005.

[72] Azad, S. K., & Hasançebi, O. (2014). An elitist self-adaptive step-size search for structural design optimization. Applied Soft Computing Journal, 19, 226–235. doi:10.1016/j.asoc.2014.02.017.

[73] Toğan, V., & Daloğlu, A. T. (2008). An improved genetic algorithm with initial population strategy and self-adaptive member grouping. Computers and Structures, 86(11–12), 1204–1218. doi:10.1016/j.compstruc.2007.11.006.

[74] Talebpour, M. H., Kaveh, A., & Kalatjari, V. R. (2014). Optimization of skeletal structures using a hybridized ant colony-harmony search-genetic algorithm. Iranian Journal of Science and Technology. Transactions of Civil Engineering, 38(C1), 1.

[75] Gholizadeh, S., Razavi, N., & Shojaei, E. (2019). Improved black hole and multiverse algorithms for discrete sizing optimization of planar structures. Engineering Optimization, 51(10), 1645–1667. doi:10.1080/0305215X.2018.1540697.

[76] Hasançebi, O. (2008). Adaptive evolution strategies in structural optimization: Enhancing their computational performance with applications to large-scale structures. Computers and Structures, 86(1–2), 119–132. doi:10.1016/j.compstruc.2007.05.012.

[77] Hasançebi, O., & Erbatur, F. (2002). On efficient use of simulated annealing in complex structural optimization problems. Acta Mechanica, 157(1–4), 27–50. doi:10.1007/BF01182153.

[78] Rahami, H., Kaveh, A., Aslani, M., & Asl, R. N. (2011). A hybrid modified genetic-nelder mead simplex algorithm for large-scale truss optimization. International Journal of Optimization in Civil Engineering, 1(1), 29-46.

[79] Talatahari, S., Gandomi, A. H., & Yun, G. J. (2014). Optimum design of tower structures using Firefly Algorithm. Structural Design of Tall and Special Buildings, 23(5), 350–361. doi:10.1002/tal.1043.

[80] Dehghani, A. A., Hamzehei-Javaran, S., Shojaee, S., & Goodarzimehr, V. (2024). Optimal analysis and design of large-scale problems using a Modified Adolescent Identity Search Algorithm. Soft Computing, 28(17–18), 9405–9432. doi:10.1007/s00500-024-09689-w.

[81] Gandomi, A. H., Talatahari, S., Yang, X. S., & Deb, S. (2013). Design optimization of truss structures using cuckoo search algorithm. Structural Design of Tall and Special Buildings, 22(17), 1330–1349. doi:10.1002/tal.1033.